Journal of Power Sources 185 (2008) 747–753

Contents lists available at ScienceDirect

Journal of Power Sources

journal homepage: www.elsevier.com/locate/jpowsour

The effect of oxygen reduction on activated carbon electrodes loaded with manganese dioxide catalyst

Narah Ominde[a], Nick Bartlett[a,1], Xiao-Qing Yang[b], Deyang Qu[a,*]

[a] Department of Chemistry, University of Massachusetts Boston, 100 Morrissey Blvd., Boston, MA 02125-3393, United States
[b] Chemistry Department, Brookhaven National Laboratory, Upton, NY 11973, United States

ARTICLE INFO

Article history:
Received 18 June 2008
Received in revised form 22 July 2008
Accepted 23 July 2008
Available online 31 July 2008

Keywords:
Design-of-experiment
Oxygen reduction
Gas-diffusion electrode
Manganese oxide catalyst
Catalytic activity

ABSTRACT

The statistical design-of-experiment method was used to identify the significant factors for making a manganese oxide-loaded activated carbon matrix. The carbon matrixes, which were made by reacting $KMnO_4$ with carbon material, were tested as gas-diffusion electrodes for oxygen reduction. Three factors—$KMnO_4$ concentration, reaction temperature, and reaction duration were tested in a two-level full-factorial design-of-experiment. The modification of carbon morphology and its effect on the performance of oxygen reduction are discussed. Temperature, $KMnO_4$ concentration, and the interaction between temperature and reaction time were found to have a significant influence on the catalytic activity of the manganese oxide-loaded carbon electrode.

1. Introduction

The search for clean and renewable power sources has been a major technological and environmental activity for several decades. Among the power sources being studied are primary and secondary battery systems, and a new generation of systems to be based on hydrogen fuel.

Air cathode has been widely used in energy conversion technologies, such as fuel cells and metal–air batteries. For example, zinc–air batteries have been used as hearing-aid batteries for more than 50 years and are currently sold for more than 500 million dollars a year worldwide [1]. Metal–air batteries and fuel cells have high energy density because the oxygen in the air is used as the active material in the cathode. Among the non-noble catalysts used in oxygen reduction reactions (ORRs), manganese oxide seems to be the most promising and widely used catalyst in an alkaline electrolyte because of its abundance, low cost, and high catalytic activity. Manganese oxides have also been extensively used as active material in the cathode in various battery systems, most notably primary alkaline MnO_2/Zn batteries.

ORR electrocatalyzed by manganese oxide was believed to occur through successive two-electron process with HO_2^- as intermediate. The reaction involves the reduction of O_2 to HO_2^- mediated by the Mn(IV)/Mn(III) couple, and MnO_x facilitates the HO_2^- intermediate species to disproportionate into O_2 and OH^- [2–6]. The catalytic activity of MnO_2 is closely related to its morphology and crystal structure, which rely on the catalyst synthesis and gas-diffusion electrode (GDE) making procedures. There are two different approaches to incorporate manganese oxide catalysts into the carbon support: mechanical mixing in which the manganese oxide catalysts are first prepared through various methods and then mixed with carbon support materials; or impregnation in which soluble Mn species in the solution are used as starting material, for example, soluble Mn(II) ions were first adsorbed into carbon support and manganese was oxidized to its high oxidation states through subsequent treatments. The advantage of the first approach is that the crystal structure of manganese oxide can be well-controlled; therefore many MnO_x-based alkaline air cathodes reported in the literature for ORR mechanistic studies were fabricated by mixing MnO_2 with high-surface area porous carbon materials [7]. However, the performance of these kinds of air cathodes largely relies on the homogeneity, uniformity, and conductivity of the matrix. Unfortunately, it is difficult to form a matrix of homogenous mixture between MnO_x and high-surface area carbon during bulk powder processing; the poor distribution of MnO_x in the carbon matrix results from the mechanical mixing of the two solid powders which have significantly different bulk densities.

* Corresponding author. Tel.: +1 617 287 6035; fax: +1 617 287 6185.
E-mail address: deyang.qu@umb.edu (D. Qu).
[1] Summer intern from Lexington Public School, currently with the School of Engineering and Applied Science, University of Pennsylvania.

0378-7753/$ – see front matter © 2008 Elsevier B.V. All rights reserved.
doi:10.1016/j.jpowsour.2008.07.065

Therefore, a high percentage of manganese catalyst may be needed to ensure high catalytic activity for ORRs [7,8].

The impregnation method is favored over mechanical mixing to achieve homogenous, highly dispersed catalyst distribution on the surface of high-surface area carbon electrodes, because uniform distribution of catalyst can be achieved more efficiently. Indeed, the impregnation method is preferred at the industrial production level, as seen in the method of MnO_2 preparation by reacting potassium permanganate ($KMnO_4$) with high-surface area active carbon material [9,10]. The permanganate is reduced by carbon mostly to MnO_2, and the forming MnO_2 catalyst is very uniformly distributed on the surface of carbon matrix. The important issues are the effects of $KMnO_4$/carbon reaction on the porous structure of carbon and its influence on the performance of the air cathode. The purpose of this work was to investigate such effects.

2. Experimental details

2.1. Materials

The high-surface area activated carbon material was purchased from Calgon, subsequently thermo-treated at 900 °C in a tube furnace under inert gas and reflux washed with acetone for 10 h. ACS grade (99.0% min) $KMnO_4$ was purchased from VWR.

Various kinds of MnO_2-loaded carbon materials were prepared by reacting $KMnO_4$ solution with carbon. 200 mL water was first poured into a 500-mL beaker, and 50 g of carbon was slowly added into the beaker with continuous stirring. After reaching the preset temperature, 80 mL of $KMnO_4$ of certain concentration was slowly added to the beaker and the reactor was kept at the preset temperature for different durations. The MnO_2-loaded carbon material was then recovered using a Buchner filter funnel. The solid was washed three times with deionized (DI) water and dried overnight in a 120 °C oven.

2.2. Electrolyte, reference and counter electrodes

Aqueous potassium hydroxide solution (30 wt.%) was used as the electrolyte in all experiments at 298 ± 2 K. All potentials reported were referred to the Hg/HgO reference electrode immersed in the KOH solution of the same concentration as the experimental electrolyte. A nickel mesh was used as counter electrode.

2.3. Construction of GDE and electrochemical cell

The GDE was made with 90 wt.% of catalyst-loaded carbon material and 10 wt.% of Teflon dry material. The Teflon suspension (T-30) used was from DuPont. The catalyst-loaded activated carbon was first wet with *iso*-propanol solution and then mixed thoroughly with T-30. The dough was subsequently hot-rolled into a thin film and then hot-pressed onto a Ni-mesh current collect using a hydraulic press.

Details of the construction of the electrochemical cell were reported previously [11]. The interfacial area between the GDE and the electrolyte was 95 mm^2.

2.4. Analysis of MnO_2 content in the loaded activated carbon

The MnO_2-loaded activated carbon material was first digested in 10% HNO_3 solution at boiling temperature. MnO_2 was then reduced to soluble Mn^{2+}. The Mn^{2+} concentration in the solution was measured using inductively coupled plasma (ICP).

2.5. Experimental techniques and instrumental details

Electrochemical measurements were carried out using an EG&G 173 potentiostat–galvanostat controlled by a Q&R Smart Data Package. A Micromeritics ASAP 2020 porosimeter was used for measuring the surface area and porosity. Nitrogen was used as an absorbate gas. Density functional theory (DFT) software from Micromertices was used for the calculation of pore distribution. Slit pore geometry was assumed. A Perkin-Elmer Optima 3000XL Inductively Coupled Plasma Spectrometer was used for the analysis of soluble Mn^{2+}. The statistical software MINITAB was used for the design-of-experiment design and data analysis.

2.6. Design-of-experiment

Design-of-experiment helps to screen the multiple factors and determine which are important for explaining process variation and how factors interact and drive the process.

Factorial designs [12] enable the investigation involving multiple factors. Instead of the traditional experimental approach, or one-factor-at-a-time method, in which one parameter is changed while the other parameters are kept constant, several factors are allowed to vary simultaneously in factorial design. Unlike the single-factor experiment, factorial design-of-experiment can reveal not only the effects of individual factors but also their interactions, which can be studied. To perform a general factorial design, a fixed number of "levels" for each of a number of variables (factors) are chosen. Then, experiments with all possible combinations are run. The responses to the change of factors are analyzed using analyses of variance (ANOVA), which are used to uncover the interactive nature of reality, as manifested in higher order interactions. Although the factorial design is unable to cover entire ranges of all factors, it can indicate major trends. To determine the effect of each factor in a multiple variant environment, design-of-experiment is frequently used in the early stage of product development to determine a promising direction for further experimentation. It is also a good practice in fundamental scientific research to use a preliminary experimental effort to look at a large number of factors superficially rather than a small number thoroughly, so that the "big picture" is not missed. Although design-of-experiment does not reveal the underlying intrinsic scientific causes for the trends, it can pinpoint the significant factors, on which the mechanistic research should be focused [13].

The factors chosen to vary in this experiment were the most critical ones for the synthesis of MnO_2-loaded activated carbon material. A two-level full-factorial design (2^3) was used for the study. All possible combinations of the levels of factors were tested with three replicates. $KMnO_4$ concentration, reaction temperature, and reaction duration were chosen as the factors to vary. The details of the two-level factorial design are listed in Tables 1 and 2. The samples were synthesized following the run order. The physical properties, such as surface area and pore distribution, and electrochemical performance of ORR were studied for each individual sample.

Table 1
Values of the three factors at two levels

Factors	Value of variable	
	Low level (−)	High level (+)
A: $KMnO_4$ concentration (%)	2	10
B: reaction temperature (°C)	22	80
C: reaction duration (min)	10	40

Table 2
Test matrix and run order for the two-level full-factorial design

Run order	$KMnO_4$ concentration (%)	Temperature (°C)	Time (min)
1	10	22	40
2	2	80	10
3	2	22	40
4	10	22	10
5	10	80	40
6	10	80	10
7	2	80	40
8	2	22	10

3. Results and discussion

3.1. Surface area and pore distribution of the MnO_2-loaded carbon material.

Given that electrocatalytic reaction is a surface phenomenon and only Mn on the surface would participate in the reaction, the accessible Mn species would be proportional to the catalytic activity. The MnO_x catalyst activity, therefore, is largely attributed to the surface area and surface defect of both MnO_2 and carbon. The surface area of a given mass of solid material is inversely related to the average pore width. The larger the surface area, the larger the percentage of small pores will be. The surface area of a solid could be contributed by external surface and internal pore surface. External surface includes the outer surface and all the pores that are wider than they are deep. The internal pore surface comprises the surface of pores which are deeper than they are wide. Obviously, from a mass transfer standpoint, the external surface and the surface of large pores are much easier to be accessed electrochemically than those of small pores. Therefore, it is very important to design the gas-diffusion electrode in such a way that the electrolyte can penetrate into but not over-flood it. A porous morphology and its interconnected pores have to provide sufficient three-phase reaction zone and diffusion paths for both electrolytes and air.

Table 1 details the values of the three factors at two-level (2^3) full-factorial design. The low and high levels of the factors were chosen wide enough to demonstrate statistical differences but within the range of practical feasibility. Table 2 tabulates the test matrix for the factorial design. Eight MnO_2-loaded activated carbon materials were prepared under the described conditions. The percentage of MnO_2, surface area, pore distribution, and electrochemical performance for ORR were measured for the eight samples and the blank carbon material.

Table 3 tabulates the percentage of MnO_2, average pore width, total surface area, and the surface area of the pore with widths less than 7 Å, 15 Å, and >15 Å. As the catalyst-loaded carbon contains MnO_2, the density of which is higher than that of carbon, the surface area of the composite and the surface area of the carbon in the composite are listed separately. The surface area of MnO_2 was assumed to be about 50–100 $m^2\ g^{-1}$. It should be emphasized that the determination of the actual surface area of the MnO_2 formed in the pores of the carbon material is difficult, the assumption is based on the fact that the surface area of commercial electrolytic manganese oxide (EMD) is about 30–50 $m^2\ g^{-1}$ [14], and the surface area of the MnO_2 synthesis from oxidation of Mn^{2+} by bubbling O_2 [15] and by $KMnO_4$ [16] was about 20 $m^2\ g^{-1}$ and 80 $m^2\ g^{-1}$, respectively. DFT was used to calculate the surface area and the pore width distribution. The traditional BET method was avoided, because it can significantly over-inflate the surface area for the microporous materials. DFT is based on a molecular-based statistical thermodynamic theory that allows relating the adsorption isotherm to the microscopic properties of the system: the fluid–fluid and fluid–solid interaction energy parameters, the pore width, pore geometry, and the temperature.

The outcomes of the statistical analysis for the experimental results are tabulated in Table 4. The impacts of the three chosen factors and their interactions on the percentage of MnO_2, matrix

Table 3
Comparison of the percentage of MnO_2, surface area, surface area of carbon, surface area of pore <7 Å, <15 Å, and >15 Å, and average pore width

Sample	MnO_2 (%)	Surface area ($m^2\ g^{-1}$)	Surface area of carbon ($m^2\ g^{-1}$)[a]	Surface of pore <7 Å	Surface of pore <15 Å	Surface of pore >15 Å	Average pore width (Å)
1	8.2	662	717–712	400	600	62	28.4
2	2.2	740	755–754	453	675	65	28.8
3	2.1	752	767–766	463	680	72	30.6
4	7.0	723	773–770	461	665	58	28.3
5	8.7	625	680–675	300	567	58	30.3
6	8.9	714	779–774	446	652	62	28.5
7	2.0	730	744–773	446	670	60	28.7
8	2.3	726	742–740	432	665	61	28.9
AC	0	717	717	320	617	100	36.9

[a] The surface area of carbon was calculated based on the assumption that the surface area of MnO_2 is 50–100 $m^2\ g^{-1}$.

Table 4
The response from the factorial design-of-experiment to the characteristics of carbon matrixes

Factors		MnO_2 (%)	SA[a]	SA carbon	Surface of pore <7 Å	Surface of pore <15 Å	Surface of pore >15 Å	Average pore width
% of $KMnO_4$ (A)	$\alpha = 0.1$	–	–	–	–	–	–	–
	$\alpha = 0.4$	–	+	+	+	+	+	–
Temperature (B)	$\alpha = 0.1$	–	–	–	–	–	–	–
	$\alpha = 0.4$	+	–	–	–	–	–	–
Duration (C)	$\alpha = 0.1$	–	–	–	–	–	–	–
	$\alpha = 0.4$	–	+	–	+	+	–	+
Interaction	$\alpha = 0.1$	–	–	–	–	–	–	–
	$\alpha = 0.4$	–	AC	AC	AC	AC	BC	AB, ABC

'–" means no significant effect and "+" means significant effect; "AC" means the interaction between $KMnO_4$ concentration (factor A) and reaction duration (factor C).
[a] Surface area.

surface area, carbon surface area, the surface area of pores <7 Å, 15 Å, and >15 Å, and average pore width are evaluated at two alpha (α) levels. The α is the probability of rejecting the null hypothesis when the null hypothesis is really true, that is, finding a significant association when one does not really exist. It is also called the level of significance. For example, $\alpha = 0.1$ denotes finding an effect that does not really exist is 10%. In other words, if an effect is found to be significant, it would be 90% certain that it is true. It appears that the three factors and their interaction did not have significant effects to the responses at a 90% confidence level. However, it is 60% certain that $KMnO_4$ concentration would have significant effect on the surface area of the matrix; temperature would significantly influence the amount of MnO_2-loaded on the surface; reaction duration would affect both the surface area and average pore width; the combination or interaction of $KMnO_4$ percentage and reaction time would have significant effect on the surface areas as well.

In a porous solid material, pores are formed within the particles of a fine powder, the primary particles, or in the aggregated secondary particles that are formed when primary particles stick together [17]. For high-surface area carbon materials, the primary particles can be considered as molecular space where the carbon atoms form a covalently bonded three-dimensional network; and within the network, imperfect layer arrangements can be recognized. The carbon microporosity is determined by the volume elements between the carbon atoms. Not all of the porosity of an activated carbon has the same entrance dimensions [18]. More porosity is open to molecules or ions of smaller width than to those with larger width. The availability of the pores to certain species is determined by the pore openings: the pore opening has to be large enough to allow penetration of the adsorbate. Closed porosity is defined as that porosity which is not accessible to a given adsorbate. There would be two kinds of closed pores: the ones that have an opening to the exterior of the grains and the sealed-off pores. Fig. 1A shows the comparison of the pore distribution of the activated carbon and two MnO_2-loaded activated carbon materials. It appears that the reaction of $KMnO_4$ with carbon material would reduce the surface area of large pores (pores >7 Å) whereas it would increase the surface area of fine pores. The effects became more pronounced when the duration of the reaction was longer. The chemical reaction between permanganate and carbon reduces permanganate to MnO_2 and oxidizes carbon to CO_2. The physical effects of the redox reaction on the carbon surface are two fold: first, the top layer of carbon will be removed by being oxidized to carbon dioxide; second, the MnO_2 fine particles that are formed will precipitate on the surface of carbon. The chemical reaction happens only if the permanganate could reach the carbon atoms; thus the initial redox reaction happens on the external surface of the activated carbon and within the large pores through which permanganate can penetrate. As the result of the initial reaction, solid MnO_2 would deposit on the walls of the large pores which will reduce the surface area of large pores. Meanwhile, surface carbon atoms would be removed and the removal of the top carbon layers would not only open up the sealed-off pores but also widen the opening of micropores. Thus the surface area of the initially closed pores, which had not been available to N_2 adsorbate, becomes accessible to the absorbate gas.

It is worth noting that changes of porosity from sample to sample are small but significant. Additional experiments were done with various activated carbon materials in our labs, the trend that the surface of large pores was reduced and the surface area of small pore was increased after the $KMnO_4$ treatment has been consistently demonstrated. The results will be reported elsewhere. As shown in Table 4, it is above 60% certainty statistically that the response of pore surface area changes to the concentration of $KMnO_4$, time and

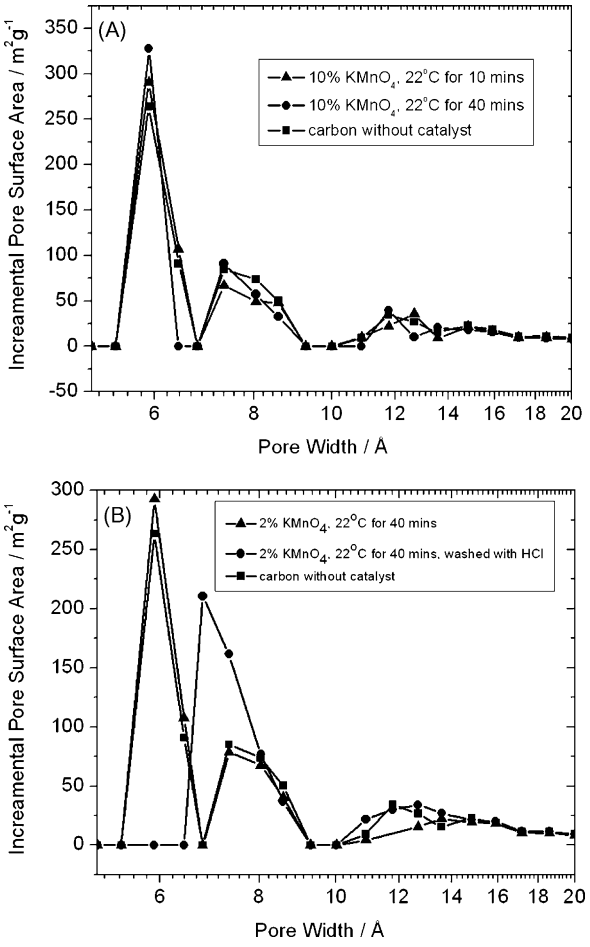

Fig. 1. Comparison of pore width distribution of blank activated carbon and manganese oxide-loaded carbon made by reacting 10% $KMnO_4$ solution with the activated carbon at 22 °C for 10 min and 40 min, respectively (A); comparison of pore width distribution of blank carbon, MnO_2-loaded carbon and the carbon with MnO_2 removed by HCl washing (B).

the interaction between the two is significant. The surface modification of carbon by $KMnO_4$ can be further demonstrated in Fig. 1B, where the pore distributions of the blank carbon, MnO_2-loaded carbon and the carbon with MnO_2 removed by HCl washing are

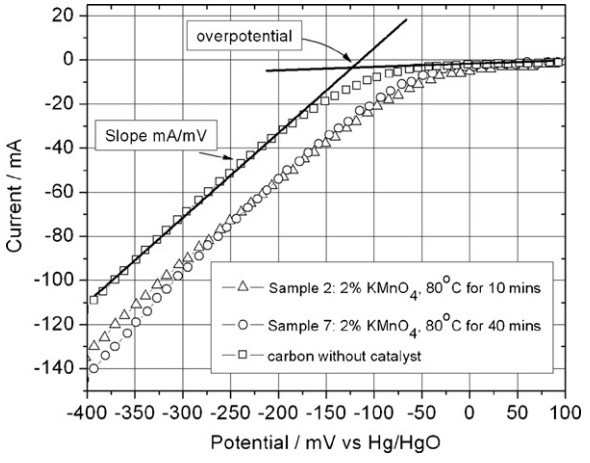

Fig. 2. Potentiodynamic for O_2 reaction at blank activated carbon and manganese oxide-loaded carbon made by reacting 2% $KMnO_4$ solution at 80 °C for 10 min and 40 min, respectively.

Table 5
Comparison of minimum overpotential and mA mV^{-1} ratio for blank carbon and eight carbon matrixes made in the design-of-experiment

	Blank	1	2	3	4	5	6	7	8
Overpotential (mV)	−146	−96.1	−70	−116	−96.2	−78.5	−68.0	−58.9	−88.6
mA mV^{-1}	0.417	0.104	0.395	0.267	0.201	0.299	0.216	0.461	0.367

compared. It is obvious that the pore width of small pores was significantly increased and more continuous pore width distribution was demonstrated.

3.2. Catalytic ORR on the surface of carbon composites

ORR is believed to undergo two successive two-electron processes with HO_2^- as intermediate. Manganese oxide was found to induce the disproportion reaction of HO_2^- to O_2 and OH^- [3]. The GDE should have sufficient sites for the ORR. This relies on the structure of the carbon material, surface porosity and the distribution of catalyst. A material with more active sites would possess higher electrocatalytic activity. Fine-sized MnO_2 catalyst well distributed in the matrix of carbon would significantly increase the number of active sites by serving introducing catalyst. Fig. 2 shows the comparison of the potentiodynamic of ORR for blank activated carbon and two manganese oxide-loaded carbon electrodes. The slope of the reduction curve in the range of high overpotential (mA mV^{-1}), as shown in Fig. 2, can be used to estimate the catalytic activity of an activated carbon electrode. The determination of reduction overpotential is also shown in the figure.

Table 5 tabulates the starting potential and mA mV^{-1} values of ORR for blank activated carbon and eight catalyst-loaded carbon electrodes. The starting potential represents the minimum overpotential for the oxygen reduction. Table 6 lists the results of the statistical analysis on the influence of the factors and their interaction on minimum overpotential and mA mV^{-1} ratio. It clearly demonstrates that the mA mV^{-1} ratio, the catalytic activity, was determined by both permanganate concentration and reaction temperature with 90% certainty. The reaction temperature had a significant effect on the minimum overpotential at the same confidence level. Even though reaction duration may not have a significant influence on both minimum overpotential and mA mV^{-1} ratio at the high certainty level, the interaction between temperature and reaction time definitely has a significant effect on mA mV^{-1} ratio. Fig. 3 shows the main effects plot for the factors with 90% confidence influence. Only the factors with high confidence as shown in Table 6 are used in Fig. 3. As shown in Fig. 3A, the catalytic activity for the ORR increases with the increase in reaction temperature and the decrease in permanganate concentration. The ORR minimum overpotential decreases as the reaction temperature increases as shown in Fig. 3B. The effect of reaction time on the catalytic activity, however, relates to the reaction temper-

Table 6
The response from the factorial design-of-experiment to the minimum overpotential and mA mV^{-1} ratio

Factors		Overpotential	mA mV^{-1}
% of $KMnO_4$ (A)	$\alpha = 0.1$	–	+
	$\alpha = 0.4$	–	+
Temperature (B)	$\alpha = 0.1$	+	+
	$\alpha = 0.4$	+	+
Duration (C)	$\alpha = 0.1$	–	–
	$\alpha = 0.4$	–	+
Interaction	$\alpha = 0.1$	–	BC
	$\alpha = 0.4$	ABC	BC

–: not significant; +: significant.

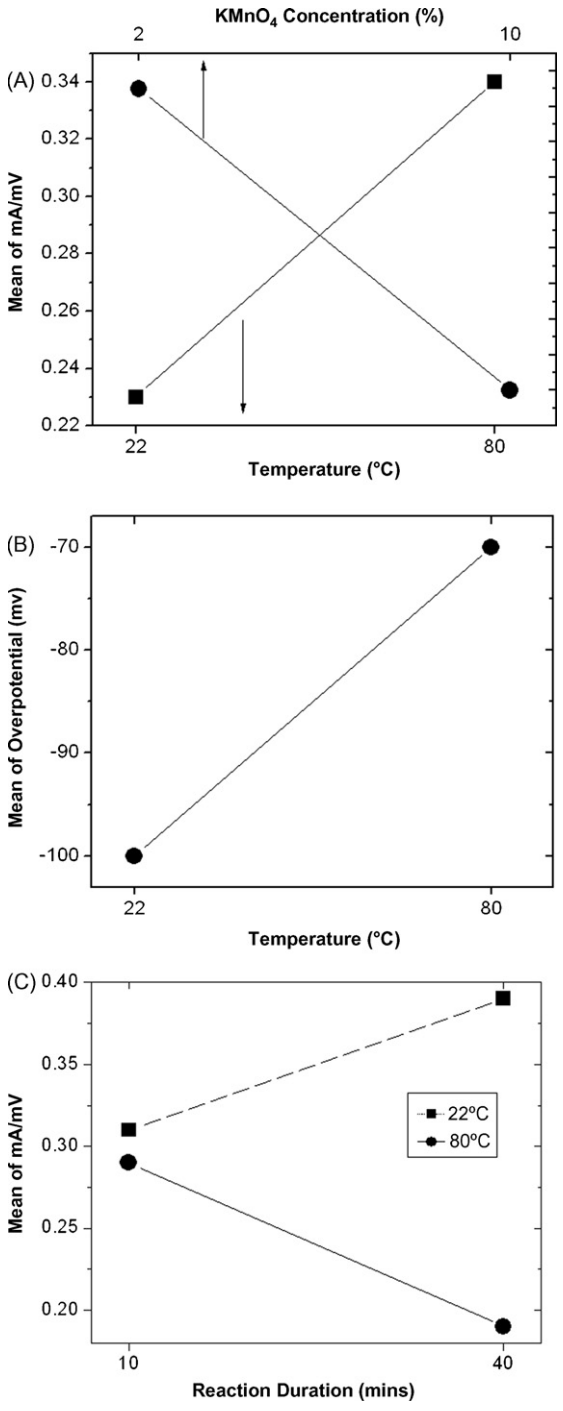

Fig. 3. Main factor plot for the effects of $KMnO_4$ concentration and temperature on the mean of mA mV^{-1} ratio (A); the effect of the reaction temperature on the mean of minimum overpotential (B); the effect of temperature and reaction duration interaction on the mean of mA mV^{-1} ratio (C). Only the significant factors are plotted.

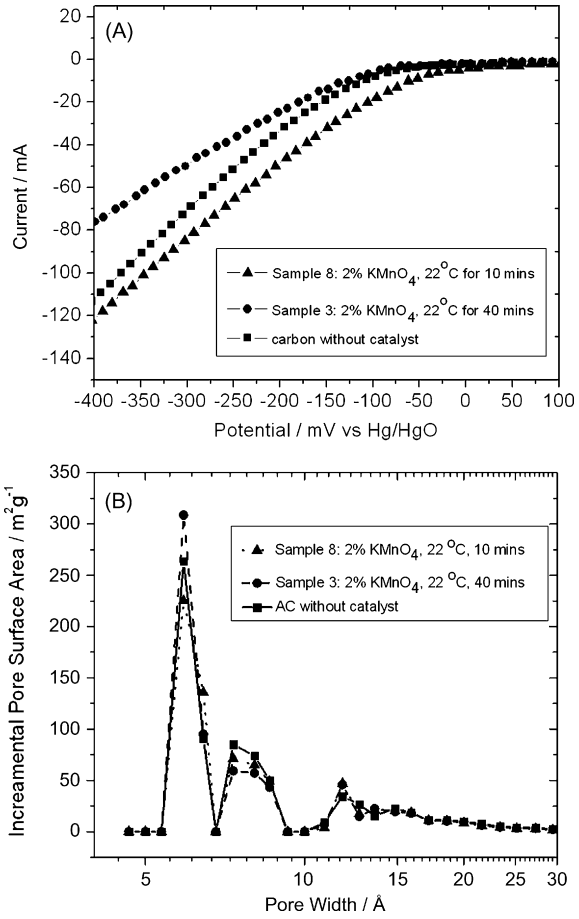

Fig. 4. Comparison of potentiodynamic for ORR on the gas-diffusion electrode made by blank carbon, carbon matrix synthesized by reacting 2% $KMnO_4$ with the carbon at 22 °C for 10 min and 40 min (A) and their pore distribution.

ature. At low temperature (22 °C), the catalytic activity increases with reaction time, whereas the reverse trend is demonstrated at high reaction temperature (80 °C). In summary, systematic statistical studies indicate that high-performance MnO_2/carbon matrix should be synthesized using a low concentration of $KMnO_4$, at high temperature for relatively longer reaction duration. Indeed, sample no. 7, which was made by reacting 2% $KMnO_4$ solution with the carbon material at 80 °C for 40 min (Table 2), demonstrated the best performance with low minimum overpotential and high catalytic activity (Table 5).

Catalytic oxygen reduction in the GDE is a surface phenomenon in which the catalytic process involves the interactions among oxygen, electrolytes, manganese oxide catalyst, and carbon support material. The number and active sites would be an important factor for the reduction kinetics. Evidentially, the carbon/catalyst matrixes made at high temperature have less minimum overpotential than those made at low temperature. The catalytic activity of manganese oxide depends strongly on the Mn oxidation state, as well as on the oxide structure. Different catalytic activities were reported for ORR on manganese oxides of different crystal structure [2,4]. It appears that the reaction temperature plays a dominant role in determining the ORR overpotential catalyzed by manganese oxides. This may be a result of the various structures exhibited by manganese oxide and the minor differences in Mn oxidation states. Owning to the low percentage of highly defect MnO_2, any possible MnO_2 diffraction peaks would be covered by the board [0 0 2] and [1 0 0] carbon diffraction peaks, an example of XRD patterns is included in online supplementary information. The hypothesis is under investigation using in situ X-ray absorption spectroscopy, which could reveal the information of short-range coordination and the change of Mn oxidation state. The results will be reported later.

The GDE structure should not only have high electronic conductivity to ensure low Ohmic resistance, but also provide a high three-phase interfacial area and a short diffusion path for quick mass transfer. The cathode with highly opened microporous structure would provide the pathway for the fast gas and electrolyte diffusion. Fig. 4 shows the comparisons of electrochemical performance and pore distribution of the blank activated carbon and the two MnO_2-loaded carbon matrixes. It seems that the minimum overpotential of catalyzed electrodes was less than that of a blank carbon electrode (also refer to Table 5). The mA mV^{-1} ratio, however, was also related to the pore distribution. The electrode with the larger percentage of big pores would have a larger mA mV^{-1} ratio than those with a small percentage of big pores. The carbon matrix with a highly open microporous structure, which could facilitate rapid mass transfer, is essential for a high-performance GDE. The ORR kinetics are related to the local current density. The larger the effective area, the lower the local current density and the faster the reaction kinetics would be. During ORR, oxygen molecules and OH^- diffuse through the network of interconnected pores and the residence times would be longer in the smaller volume elements of the porosity because of the curvature effect. This effect is more pronounced for gas-diffusion than ion diffusion. The effect occurs in pores that are narrow enough for the whole of the adsorbate to be in range of the forces originating from the solid surface. At this

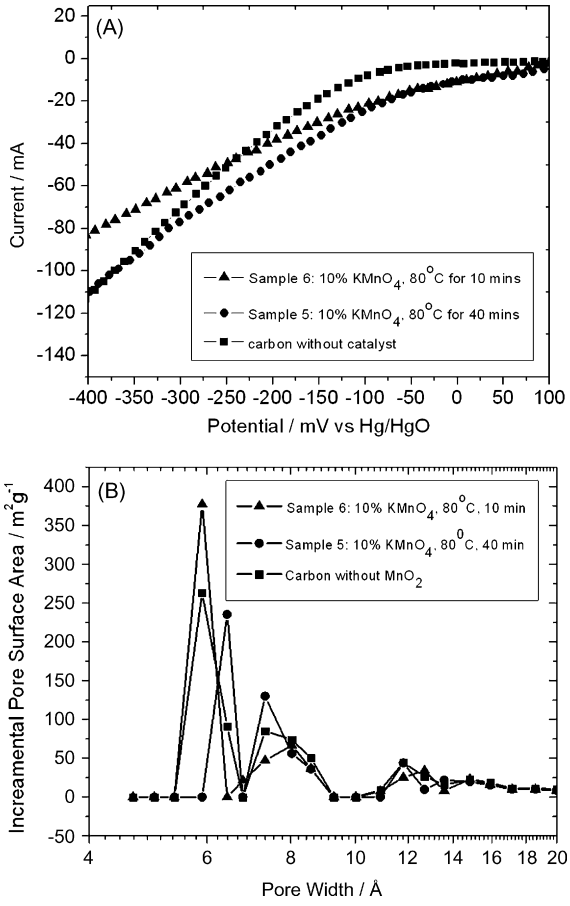

Fig. 5. Comparison of potentiodynamic for ORR on the gas-diffusion electrode made by blank carbon, carbon matrix synthesized by reacting 10% $KMnO_4$ with the carbon at 80 °C for 10 min and 40 min (A) and their pore distribution.

distance, the influence of the surface of neighboring walls would overlap, so the interaction energy of the solid with a gas molecule would be correspondingly enhanced. Such curvature effects only occur in pores with a width not exceeding a few molecular diameters [19]. The diameter of oxygen is 3.55 Å [20]. It was suggested that a pore diameter in the order of 18 Å would be required to facilitate an effective ORR and only the large pore surface should be considered as an effective reaction interface [11,21]. Therefore, even though the oxidation of a carbon surface by permanganate could make some closed pores available to N_2 adsorbate during the measurement of isotherms, those pores may not be available to ORR. However, if the surface of large pores was reduced by MnO_2 precipitation; the effective surface area for ORR would be reduced after the catalyst was loaded. This phenomenon is demonstrated in Fig. 4. Finally, Fig. 5 shows the ORR potentiodynamic profiles and the pore distribution on the manganese oxide-loaded carbon made with higher $KMnO_4$ concentration at higher temperature than those in Fig. 4. The same trend was demonstrated in Fig. 5 as that of Fig. 4. However, even though MnO_2-loaded carbon electrodes in Fig. 5 demonstrated high catalytic activity, the advantage gradually disappeared as the current increased. As shown in Table 3, the percentage of MnO_2 in samples 5 and 6 (electrodes in Fig. 5) was much higher than that in samples 3 and 8 (electrodes in Fig. 4). MnO_2 is a typical semi-conductor. In addition to the polarization resulting from both sluggish charge transfer and mass diffusion limitations would also add to that arising from a lack of catalytic sites for oxygen reduction and rate limited the oxygen supply. Ohmic IR polarization starts to play an important role as the current increases.

4. Conclusions

Systematic design-of-experiment investigation reveals the significant effects of the main factors and their interactions on the physical characteristics of manganese oxide-loaded carbon matrix and on their catalytic activities for ORR. Permanganate was believed to react with carbon material forming manganese oxide deposits and carbon dioxide. As the results of the redox reaction, some of the closed micropores were opened for the access of N_2 adsorbate during the porosity measurement because of the removal of the surface carbon layers. The surface of pores with width less than 15 Å may not be available for ORR. Manganese oxide was deposited on the external surface and the surface of large pores; the large pore surface area was reduced, which had a negative effect on ORR. A significant factor that influenced the minimum overpotential was the reaction temperature: the higher the temperature, the less the overpotential would be. It was proposed that the crystal structure of manganese oxide and the oxidation state of Mn could be different for the materials made at different temperatures. The ratio of mA mV^{-1} was significantly influenced by $KMnO_4$ concentration, reaction temperature, and the combination of temperature and reaction duration.

Acknowledgments

The work was supported by the Assistant Secretary for Energy Efficiency and Renewable Energy, Office of Vehicle Technologies, under the program of "Hybrid and Electric Systems," of the U.S. Department of Energy under Contract Number DEAC02-98CH10886. The work at UMB was also partially supported through UMB faculty start-up grant. Both financial supports are gratefully acknowledged.

Appendix A. Supplementary data

Supplementary data associated with this article can be found, in the online version, at doi:10.1016/j.jpowsour.2008.07.065.

References

[1] T. Ohsaka, L. Mao, K. Arihara, T. Sotomura, Electrochem. Commun. 6 (2004) 273–277.
[2] F.H.B. Lima, M.L.E. Calegaro, E.A. Ticianelli, Electrochim. Acta 52 (2007) 3732–3738.
[3] L. Mao, D. Zhang, T. Sotomura, K. Nakatsu, N. Koshiba, T. Ohsaka, Electrochim. Acta 48 (2003) 1015–1021.
[4] Y.L. Cao, H.X. Yang, X.P. Ai, L.F. Xiao, J. Electroanal. Chem. 557 (2003) 127–134.
[5] F.H.B. Lima, M.L.E. Calegaro, E.A. Ticianelli, J. Electroanal. Chem. 590 (2006) 152–160.
[6] M.L. Calegaro, F.H.B. Lima, E.A. Ticianelli, J. Power Sources 158 (2006) 735–739.
[7] K. Gong, P. Yu, L. Su, S. Xiong, L. Mao, J. Phys. Chem. 111 (2007) 1882–1887.
[8] Z.Q. Fang, M. Hu, W.X. Liu, Y.R. Chen, Z.Y. Li, G.Y. Liu, Electrochim. Acta 51 (2006) 5654–5659.
[9] P. Zoltowsi, D.M. Drazic, L. Votrkapic, J. Appl. Electrochem. 3 (1973) 271–283.
[10] P. Bezdicka, T. Grygar, B. Klapste, J. Vondrak, Electrochim. Acta 45 (1999) 913–920.
[11] D.Y. Qu, Carbon 45 (2007) 1296–1301.
[12] G.E.P. Box, W.G. Hunter, J.S. Hunter, Statistics for Experimenters: An Introduction to Design, Data Analysis and Model Building, John Wiley & Sons, New York, 1978.
[13] A.M. Kannan, A.K. Shukla, S. Sathyanarayana, J. Power Sources 25 (1989) 141–150.
[14] D.Y. Qu, Electrochim. Acta 48 (2003) 1675–1684.
[15] D.Y. Qu, L. Bai, C.G. Castledine, B.E. Conway, W.A. Adams, J. Electroanal. Chem. 365 (1994) 247–259.
[16] M. Andres Peluso, L.A. Gambaro, E. Pronsato, D. Gazzoli, H.J. Thomas, J.E. Sambeth, Catal. Today 133–135 (2008) 487–492.
[17] S.J. Gregg, K.S.W. Sing, Adsorption, Surface Area and Porosity, Academic Press, London, 1982.
[18] H. Marsh, F. Rodriguez-Reinoso, Activated Carbon, Elsevier, Boston, 2006.
[19] D. Qu, Chem. Eur. J. 14 (2008) 1040.
[20] CRC Handbook of Chemistry and Physics, 88th ed. (2007–2008) pp. 6–34.
[21] A.J. Appleby, J. Marie, Electrochim. Acta 24 (1979) 195–202.